Bulletin of Environment, Pharmacology and Life Sciences
Bull. Env. Pharmacol. Life Sci., Vol 11 [11] October 2022 :204-214

Online ISSN 2277-1808
Journal's URL:http://www.bepls.com
CODEN: BEPLAD

ORIGINAL ARTICLE **OPEN ACCESS**

Soil moisture and soil temperature assimilation using HRLDAS for heavy rainfall event forecasting over the Indian region

Neha Verma[1], Shivali Kundan[1], Zahid Nabi[1], Dinesh Kumar*[1]
[1]Department of Environmental Sciences, Central University of Jammu-181143, J&K, India
*Corresponding Author's Email: dkumarcuj@gmail.com

ABSTRACT
Surface fluxes such as latent and sensible heat flux are highly influenced by land surface variables. Studies have shown that partitioning of available radiation into latent and sensible heat fluxes is very much dependent on soil moisture which further affects the boundary layer depth and other associated characteristics. Therefore, the present study focused on assessing the improvement when high-gridded soil moisture and temperature data were assimilated at initial conditions using a high-resolution land data assimilation system (HRLDAS) for forecasting heavy rainfall events over highly urbanized regions in India. The results showed the increased soil moisture which mixes vertically increasing the lower atmospheric moisture. The improved CAPE along with surface fluxes i.e. latent and sensible heat fluxes were observed after assimilation which is further used to evaporate more moisture into the atmosphere. The results also suggest a significant improvement in timing and spatial coverage of the rainfall events taken which might be due to better exchanges of moisture and heat fluxes and further boundary layer development more realistically.
Key Words: *Heat fluxes, Data assimilation, Initial Condition*

Received 22.10.2022 Revised 25.10.2022 Accepted 10.11.2022

INTRODUCTION

The lower atmospheric layer near the earth's surface is affected greatly by land surface characteristics which largely determine the partitioning of available energy into latent and sensible heat flux [1]. The spatio-temporal variability of surface moisture and temperature provide the moisture through evaporation and heat the atmospheric layer near the surface shaping the atmospheric boundary layer [2]. The feedback between convective process(s) and surface moisture and temperature exists and has been less explored as indicated by many research works [3, 4]. With the proper representation of moisture and heat flux, the predictability of such events can be assessed and quantified [5]. Initializing the land surface model at a finer scale (mesoscale or less) and coupling it with the mesoscale atmospheric model can provide improved soil moisture and soil temperature as one of the land surface characteristics [6]. Previously many attempts have been done to assess the role of moisture and heat and its impacts. [2] his scaling approach and numerical simulations for cold environments showed that soil surface fluxes affect sensible heat flux resulting in significant alterations in boundary layer depth and boundary layer warming. A customized soil-vegetation parameterization scheme was applied by [7] emphasizing the better soil heat and moisture representation and its impact on the boundary layer over NW India. They observed the improvement in wind components, potential temperature, and specific humidity. The study also revealed the unpredictability of wet soil cases which represented the vegetated or wet soil surface modifying the boundary layer process. [8] pointed out the complex interplay among the factors inhibiting or favoring the convection initiation. These factors over complex and heterogeneous terrain further condition the feedback sign between soil moisture-precipitation.

Similarly, initial soil moisture perturbations affected surface heat fluxes strongly [9]. Land surface characteristics can also be represented more accurately by improving the schemes in land surface models. The inclusion of soil moisture and temperature in coupled land surface and mesoscale atmospheric model using the assimilation technique might provide more insight into the flux exchange between the surface and boundary layer. Soil moisture and temperature assimilation and its impact were attempted by [10] using a four-dimensional data assimilation technique taking Indian monsoon depression as a case study. They pointed out the improvement in surface fluxes, surface temperature, and moisture after assimilation. The assimilation improved the model performance by reducing the errors on all surface fields. [11] in coupled land surface and atmospheric model showed that the rainfall is much more sensitive to cumulus

scheme and land surface characteristics which attribute to spatial distribution and intensity of rainfall.
The necessity of accurate soil moisture retrieval and representation has been accepted by various research works [9,12,6]. Further, the conventional observational networks were unable to provide the soil moisture and other land surface variables at high spatial and temporal scales. Therefore, the updated land surface properties are required to meet with land surface models (LSM). The updated land surface properties require techniques, derived, and model data which provide the required forcing to run uncoupled updation of LSM by observed forcing condition. Data assimilation, satellite-derived soil data, and land surface models through an intermediate step can capture the spatial and temporal changes in soil moisture. Therefore, a high-resolution land data assimilation system (HRLDAS) has the capacity to provide the required land surface variables to initialize LSM. [13] and [6] assimilated the soil moisture and temperature to observe the improvements in predicting severe thunderstorms over the Indian region. The land data assimilation system (LDAS) improved the wind and moisture conditions and reproduced the convectively unstable region of the weather system. The significant improvement in rainfall intensity in LDAS was also reported in their study.
The present study is an effort to assimilate soil moisture and temperature in the mesoscale WRF Model provided by the Noah-LSM model. Further, the study also tries to investigate the influence of land surface properties such as soil moisture and temperature on surface fluxes and atmospheric boundary layer which ultimately affect the convective outcome i.e. rainfall. Land surface state (Noah-LSM) has been updated offline from high-resolution land data assimilation system (HRLDAS) output taking heavy rainfall events over Delhi, India. In the purview of the above, the objectives of this study are to [1] understand the impact after assimilation on surface variables [2] the impact on heat flux (latent and sensible [3] improvement on the spatial pattern of precipitation [4] to analyze the vertical profiles of moisture and updraft.

Description of Convective events:

The model computations and validation from observed data such as automatic weather station (AWS) have been used to analyze the heavy rainfall over Delhi, India. Four heavy rainfall events that occurred over Delhi on 12th July, 14th Aug, 6th July, and 3rd September 2010, are considered.

Case-1, 12 July2010

Fig 2a shows the synoptic condition derived from NCEP data at 00 UTC on 12 July 2010 (Case-1). An elongated low-pressure area lies from north Pakistan to west Uttar Pradesh and the trough continues to head bay through Bihar and Jharkhand. Cyclonic circulation in upper air is seen over north Punjab, west HP, Assam, and north Pakistan in lower levels. A trough from this system extends up to AP across MP and Chhattisgarh (fig-2a). Further, there is strong surface wind flow from Gujarat and Rajasthan covering up to Punjab UP and some portions of Bihar. Over the Tibetan plateau, Jet is present which is far north of the study domain.

Case-2, 14 Aug 2010

Low-pressure area extension is seen over North UP to WB in NCEP FNL derived surface pressure plots (fig-2b) at 00 UTC on 14 Aug 2010. A patch of low pressure is also observed over Rajasthan and Gujarat. 500-hPa wind is showing a trough over Uttrakhand, Gujarat, and adjoining areas. Further, the mid-tropospheric trough lies at 78° E (Fig-2b). These mid-level air circulations have nourished the genesis of the afternoon convective system which intensified at 8UTC leading to heavy rainfall of 63 mm over Delhi.

Model Description and Coupling:

WRF-ARW Modeling system:

ARW model has been used for the simulation of weather phenomena. It is a weather prediction model designed for both research and operational applications. Various features such as multiple physics options, nesting domain, and multiple portable platforms enable the ARW model to customize to simulate/forecast extreme weather events such as tropical cyclones, heavy rainfall, and severe thunderstorms. The model properties also include the Arakawa C-grid, 30 seconds model integration time step along with 51 sigma (σ) levels with the top of the model set at 50 hPa.

Where $\sigma = (ph \_ pht)/ (phs \_ pht)$, …… (1)

while ph is the hydrostatic component of the pressure, and phs and pht refer to values of the pressure along the surface and top boundaries, respectively.

High-Resolution land data assimilation system (HRLDAS):

HRLDAS is a land surface modeling system that updates soil state variables in the Noah Land surface model (Noah LSM) in uncoupled mode. It models the evolution of land and soil parameters by integrating fine static surface fields such as land use and soil texture maps, satellite-derived vegetation parameters such as green vegetation fraction, observed rainfall, and solar downward radiation at the surface. Some weather parameter analyses from the Model and observation is also integrated into HRLDAS to capture the long-term evolution of land-state variables (e.g., soil moisture and temperature profiles). Since the

land surface variables in Noah-LSM are updated with HRLDAS, the atmospheric model i.e. WRF should use the same land surface model parameters as it is been updated with HRLDAS. In order to meet above mentioned requirement HRLDAS is run on the same model grid (nested domain). Running HRLDAS on the same nested domain enables HRLDAS soil conditions to be updated and be used for coupled WRF–Noah model without interpolation. Moreover, uncoupled HRLDAS is completely compatible with the WRF–Noah coupled model.

Noah Land Surface Model:

The Noah LSM is part of the National Centers for Environmental Prediction (NCEP) to predict weather and climate in operational mode. Noah contains a total soil depth of two meters and the lower boundary condition of soil moisture is gravitational-free drainage at the model bottom. Noah-LSM didn't allow much infiltration of snow melt water into the soil because frozen soil is significantly resistant under most vegetation and climate conditions. [14] has listed the recent updates to the Noah LSM as soil thermal conductivity treatment and ground heat flux for wet soils and snowpack along with bare-soil evaporation formulation. A simple urban land use treatment and seasonal variability of surface emissivity [15] were also included. Because LSMs provide the surface boundary condition to the atmosphere, LSPs play critical roles in affecting the PBL structure. In addition, due to the development of mesoscale meteorology modelings (MMMs) with higher spatial and temporal resolutions, it is very important to obtain the land surface forcing at a small scale (e.g. soil moisture, soil temperature, vegetation type, soil characteristics). Therefore, much attention is devoted to the parameterization of the PBL in MMMs [16, 17, 18, 19].

MATERIAL AND METHODS

Methodology and Numerical Experiments:

Nested (Two) domains are used; the outer domain of 9 km and the inner nested domain of 3 km horizontal resolution have been used (fig-1). The outer domain covers 73E -81E and 24N -32N, while, inner nested domain covers 74.9˚E – 79.2˚E and 25.8˚N – 30˚N. Table-1 gives a brief illustration on the model configuration used for the present study. NCEP-FNL data (in 6-h interval of .25◦ * .25◦ horizontal resolution) were used to initialize the control simulation (CNTL) without assimilation of soil moisture/temperature. While in the HRLDAS experiment (namely LDAS) the model IC (initial condition) was updated by ingesting soil moisture and temperature obtained from HRLDAS. Using un-coupled HRLDAS high spatio-temporal resolution of soil moisture and soil temperature profile observations were estimated at (0–10 cm, 10–30 cm, 30 cm–1 m, 1–2 m) depth for parent and nested domain. MERRA reanalysis (0.5 ◦ × 0.67 ◦) data were used as atmospheric forcing while TRMM-3B42-V7 (0.25 ◦ ×0.25 ◦ and 3-hourly) data were used as rainfall forcing. MERRA data were interpolated using the bi-linear method to keep zonal and meridional directions the same (0.5 ◦ × 0.5 ◦). Offline LDAS was run for 10 years so that the model attains equilibrium. USGS was used to obtain land surface variables such as vegetation, soil type, land use, and, land type. LDAS were initialized using GLDAS analysis of NCEP. The model configuration remains the same for CNTL and LDAS experiments. Model simulated rainfall is validated with TRMM accumulated rainfall and AWS observation.

RESULTS AND DISCUSSIONS

The simulation results of thunderstorm cases were analyzed for all four cases. Improvements in initial conditions after the assimilation of soil moisture and soil temperature are analyzed and the impact on model simulation is evaluated further.

Soil moisture/temperature improvement at the initial time:

The goal of HRLDAS is to provide improved surface land state variables (soil moisture, temperature) to initialize coupled WRF-Noah system. Improved initial conditions are crucial for NWP forecast [20]. Forecast accuracy/error is very sensitive to initial condition improvement/error mostly in cloudy and rainy regions [21]. Fig-3 shows the soil moisture and temperature increments in CNTL and LDAS experiment. From Fig: 3-b it is seen that most of the regions had shown a positive increment after the moisture assimilation, however, the south-western part has gained significant moisture in the range of 0.15-0.18 m^3 m^{-3} in LDAS in case-1. On the contrary, the north-western and south-eastern parts became drier in the LDAS experiment in case-2 (Fig-3d). Further, it was observed in both cases that moisture had increased in the range of .03-.09 m^3 m^{-3} over the area where the thunderstorm occurred, in the LDAS experiment. On the other hand, soil temperature decreased and the soil became wetter in LDAS experiments in case-1 and case-2. The vertical profile of wind magnitude (ms-1), mixing ratio (kg kg-1), and equivalent potential temperature (K), at initial conditions over Delhi is presented in Fig-4. Initial improvement in vertical profiles of moisture and temperature provided a platform to evolve the atmospheric condition. Equivalent potential temperature (Θe) and mixing ratio are important variables to

address the positively buoyant air at low levels in the atmosphere. Θe is a very useful variable to identify the most positively buoyant air and is used to represent the combined influence of high temperature and humidity at low levels in the atmosphere. When the equivalent potential temperature becomes high at a lower atmosphere (at 700 hPa), it indicates the development of violent deepening resulting in lower MSLP (<925 hPa) (22). Therefore, theta-e ridges indicate the initiation of the convective event which is thermodynamically induced thunderstorms. Increased Theta-e as much as 363-361 K were extended up to the 800-hPa (Fig-4c) which was also accompanied by an elevated mixing ratio in the range 20-16.7 kg kg-1 (Fig4b) in case-1. LDAS had simulated increased lower atmospheric moisture (16-11 kg kg-1) and region with high Theta-e (362-353 K) up to 850-hPa which was closer to radiosonde observation compared to CNTL (Fig4b&c) in case-1. Tough wind variation through all levels was unable to reproduce, vertical pattern had been improved in LDAS. Radiosonde observation over Delhi showed that wind fluctuates from stronger to weaker up to 100 hPa which is reported with good agreement in LDAS (Fig-4a). However, CNTL had failed to capture the strong wind at mid-level (600-500 hPa). Atmospheric properties in LDAS had improved which might be because of better fluxes and moisture progress and resulted in better initial vertical atmospheric variables.

Progression of CAPE, rainfall and temperature (2m):

Conditional instability helps to develop deep convection along with availability of moisture. Differences among the air masses in terms of temperature and humidity trigger the development of unstable atmosphere leading to development of the thunderstorm [23]. One of the examples of such indices is Convective Available Potential Energy (CAPE) and it represents the energy directed vertically acting upon air parcel. The threshold limit of CAPE for super-cells to form is >1500 J kg−1 [24]. Therefore, the model simulated CAPE (J/kg) is derived and compared with those of available six hourly FNL observations. Fig-5 illustrates the time series of CAPE and air temperature for case-1 and case-2. Time series showed that CAPE in LDAS in good agreement with observed CAPE except at the time of convection. In case-1 and case-2, the LDAS simulated the maximum CAPE i.e. 1554 J kg−1 and 2253, J kg−1 264 at 13 UTC and 10 UTC respectively (Fig: 5-a & 5-d). Although CNTL had shown CAPE evolution similar to LDAS, the time error and intensity were more. Thus, LDAS simulated a convective atmosphere over Delhi closer to the actual occurrence of heavy rainfall events as compared to the CNTL. It is evident that assimilation has produced unstable atmospheric development with high CAPE which might have acted as a platform to develop the severe convection. Rainfall evolution for the 24-hour duration has been depicted in Fig-5-b & 5-e. Rainfall in the range of 50 mm at 14UTC and 63 mm at 10 UTC were observed in case-1 and in case-2 respectively. Significant improvements in rainfall evolution in terms of time lag are evident in LDAS. Rain in LDAS had progressed very much as observed in both cases as compared to CNTL. Though LDAS overestimated (underestimated) the rainfall in case-1 (case-2), time error was significantly reduced. Moreover, LDAS had captured another convective condition at 21UTC associated with moderate rain in case-2 except 10UTC convective event. It is well known that surface precipitation leads to a decrease in air temperature. [25] have found that surface temperature is a very useful parameter in forecasting the occurrence of a thunderstorm. The observed temperature had shown 8° c and 6° c drop at 14UTC and 10UTC in case-1 and case-2 respectively. LDAS simulated a similar progression of temperature in both cases as compared to the CNTL experiment.

Progression of soil moisture, soil temperature, sensible heat flux, and latent heat flux:

Surface heat fluxes are computed in coupled-mode models using high-quality soil conditions provided by HRLDAS. The moisture and air temperature lying between the upper boundary surface and atmosphere influence the increase or decrease in sensible and latent heat fluxes at the upper boundary [26,27]. Fig-6 shows the surface variables like soil moisture, temperature, sensible heat flux, and latent heat flux are depicted. Surface variables are explained on the basis of occurred rainfall and air temperature due to the unavailability of surface observation. LDAS provided increased moisture (0.26 m3 m-3 at 0UTC) and reduced temperature (302 K at 0UTC) right from the beginning which was attributed to the increased surface evaporation (Fig: 6-a & b). The evaporation had left less energy to warm the soil resulting in cooler soil and a weaker sensible heat flux which can be seen in Fig: 7-b and 7-d. Latent heat flux was larger (max 292 Wm-2 at 8UTC) during the daytime because of increased air temperature, but decreased at night due to lack of solar radiation. Weaker sensible heat flux in LDAS was because of evaporation which is attributed to an increase in air temperature (2m) (Fig-5-c). The increased soil water content after rain influences sensible and latent heat flux through evaporation. Soil moisture has increased exponentially after the rain at 14UTC in LDAS for case-1 (Fig: 6-a). Rainfall provided sufficient moisture which may lead to the consumption of a substantial fraction of available surface energy for evaporation. It had been found that latent heat flux and sensible heat flux have anti-correlation i.e. during increased latent heat flux, sensible heat flux decreased [28]. Although LDAS had simulated increased soil moisture from the beginning in case-2 also, increased moisture is more at the time of rain i.e. 9UTC and 12UTC.

Surface heat fluxes were similar in LDAS and CNTL before the rain as it was seen that sensible heat flux was stronger at lower moisture content. After the rain, soil temperature was reduced by 2-3 c due to evaporation which is also seen in heat flux plots (Fig: 6-g &6-h). Though sensible and latent heat flux in LDAS variation was small after the rain, it improved significantly as compared to CNTL in case-2. From the analysis of surface variables, it is evident that LDAS had shown a better evolution of moisture and heat fluxes based on rainfall progression as compared to CNTL.

Analysis of vertical velocity, moisture convergence, and mixing ratio:

The vertical structure of moisture convergence for the 24 hours for case-1 (fig-7) revealed that the moisture convergence in CNTL started to build up from 12UTC and became strong at 16UTC UTC extending up to about 750 hPa. CNTL simulated the thunderstorm activity after the observed time. However, the LDAS had simulated a strong convergence peak up to 500 hPa at 14UTC which was closer to the observed time of occurrence. Initial positive soil moisture increment in LDAS had progressed into increased moisture availability in the thunderstorm area during the forecast hours. Though the moisture convergence was weaker in case-2, the time of occurrence had improved in LDAS. It is thus, observed that LDAS simulated the time of occurrence of convection initiation closure to observation as compared to CNTL. Updraft speed gives an insight into the intensity of convection which has been found in many findings. Studies have found that intense storm possesses a stronger convective updraft signature which carried more ice into anvils [29]. Further, damaging and hazardous winds are identified on the basis of downdraft intensity [30]. Furthermore, the existence of strong updrafts and downdraft side by side is considered an indication of severe thunderstorm occurrence. Low-level moisture convergence supported by strong upward vertical velocity provides more possibility of deep convective events occurring when the atmosphere is forced unstable. The time-height evolution of vertical velocity (cm s^{-1}) for case-1 captured a strong updraft (25-110 cm s-1) up to 200 hPa at 14-15 UTC in LDAS. Moreover, LDAS had shown strong updraft (25-110 cm s-1) in case-2 also. It is pretty much evident that vertical velocities became better in LDAS. The model simulated significant moisture at the lower atmosphere in LDAS and CNTL in case-1. But, moisture peak at the time of convection i.e. 14UTC was more pronounced in LDAS as can be seen in fig-7 for case-1. Further, case-2 was simulated a little drier compared to case-1 and LDAS provided more deep moisture at the time of convection i.e. 9UTC. Though moisture was simulated at a lower atmosphere at 6-10UTC in both LDAS and CNTL experiments, LDAS provided the intensity and moisture availability at the right time in case-2. It was observed that the mixing ratio has increased significantly in LDAS at respective updrafts in case-1 and case-2. More moisture in the lower levels accompanied by strong updraft was evident particularly in LDAS compared to CNTL. The right unstable vertical warm air column after assimilation was captured probably due to the combined effect of upward latent and sensible fluxes from the underlying warm land surface and the strong updrafts in the convective region.

Rainfall simulation:

Six hourly accumulated rainfall is validated with TRMM (fig-8). Studies have revealed that the accuracy of the TRMM data decreases at small (<1mm) and very high (>80mm) rainfall (31, 32). The Northeast and northwest parts of Delhi showed 80mm of rain in case-1(fig-8a) while it was the northern part that got 60mm of rain in case-2 (8b) in TRMM observation. Scattered patches mostly in the north-western part showed 60 mm of rain in case-3 (Fig-8c) and case-4 (fig-8d) gained 50 mm of rain in the northeastern part of Delhi. The spatial distribution of the rainfall was similar to TRMM observation in all the cases except case-2. But, it is the LDAS that had intensified and spread the rain closer to the observation. It is evident that LDAS rainfall had improved due to the better exchanges of moisture and heat fluxes with the assimilation of soil moisture/temperature leading to boundary layer evolution realistically. Moreover, the overall better representation of rainfall in LDAS may be because of the reduced time error and better spatial positioning of thunderstorm activity.

CONCLUSIONS

To study the role of land surface parameters like soil moisture and soil temperature on the genesis and evolution of heavy rainfall, analysis of soil moisture/temperature, vertical profiles of wind speed, mixing ratio, and Theta-e were carried out at the initial condition (00UTC). The simulations were done with a WRF-Noah coupled model, initialized by the use of a high-resolution land surface data assimilation system (HRLDAS). Analysis has shown that soil moisture has increased and the soil temperature has decreased over the region of interest in the LDAS experiment.

Initial improvement in vertical profiles of moisture and temperature provides a platform to evolve the atmospheric condition better. LDAS has simulated increased lower atmospheric moisture and region with high Theta-e at the lower region which is also observed in radiosonde observation. Conditional instability of the atmosphere increases with the moisture influx into the lower atmosphere which leads to latent heat

release (i.e. precipitation). The lower atmosphere has gained more converging moisture, particularly in the LDAS experiment along with enhanced vertical velocity. A significant reduction in time error of the actual occurrence of thunderstorms was observed after assimilation. LDAS simulation also improved air temperature (2m), CAPE, and rainfall. Surface variables like soil moisture, soil temperature, and sensible and latent heat flux have progressed in a better possible realistic pattern. Assimilating the soil moisture and temperature may have influenced surface evaporation resulting in cooler soil, weaker sensible heat flux, and stronger latent heat flux. One of the other reasons for higher latent heat flux during the daytime may be the presence of solar radiation. Rain may also significantly influence the sensible and latent heat flux through increasing soil water content. The spatial distribution of model simulated 6-hour accumulated rainfall in LDAS is also in better agreement with TRMM observation.

Initial land surface variables assimilation and improvements afterward in moisture and heat fluxes could have provided a better platform for the evolution of the boundary layer realistically. The improvement after assimilation might be better exchanges of moisture and heat fluxes which had led to boundary layer development more realistically. Overall better representation of rainfall in LDAS may be because of the reduced time error and better spatial positioning of thunderstorm activity. Further, even though LDAS shows overestimation/underestimation of rainfall, the time error is significantly reduced. The above discussion suggests that the assimilation of soil moisture and soil temperature influenced the surface variables' progression in a better way resulting in more realistic boundary layer development and finally capturing improved thunderstorm activity.

Table-1: Model configuration used in the present study.

Model Configuration		
Time step for Integration (s)	30	
Number of Domains	2	
East-west Dimension	100	166
South-north Dimension	111	172
Vertical Levels	51	
Grid Distance in X-direction in m	9000	3000
Grid Distance in Y-direction in m	9000	3000
X-coordinate of the lower left corner	1	23
Y-coordinate of the lower left corner	1	27
Grid ratio	1	3
LDAS Experiment		
Microphysics Option	WSM-6 class Graupel Scheme	
Long wave radiation Option	GFDL (eta) Long wave shortwave radiation	
Short wave radiation Option	GFDL (eta) Long wave shortwave radiation	
Land surface Option	Unified Noah Scheme (NOAH)	
Planetary Boundary option	MYJ (Mellor-Yamada-Janjic (eta)TKE scheme)	
Cumulus Parameterization option	Kain-Fritsch scheme (KF)	

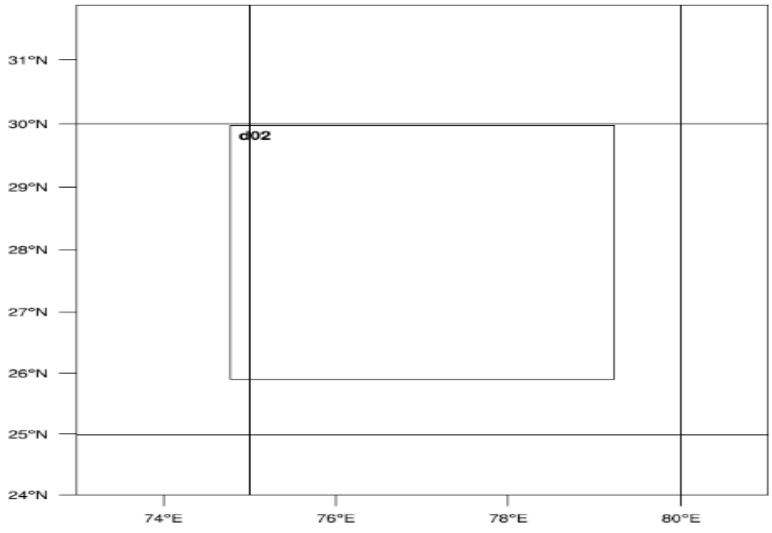

Figure 1: Model domain used for study

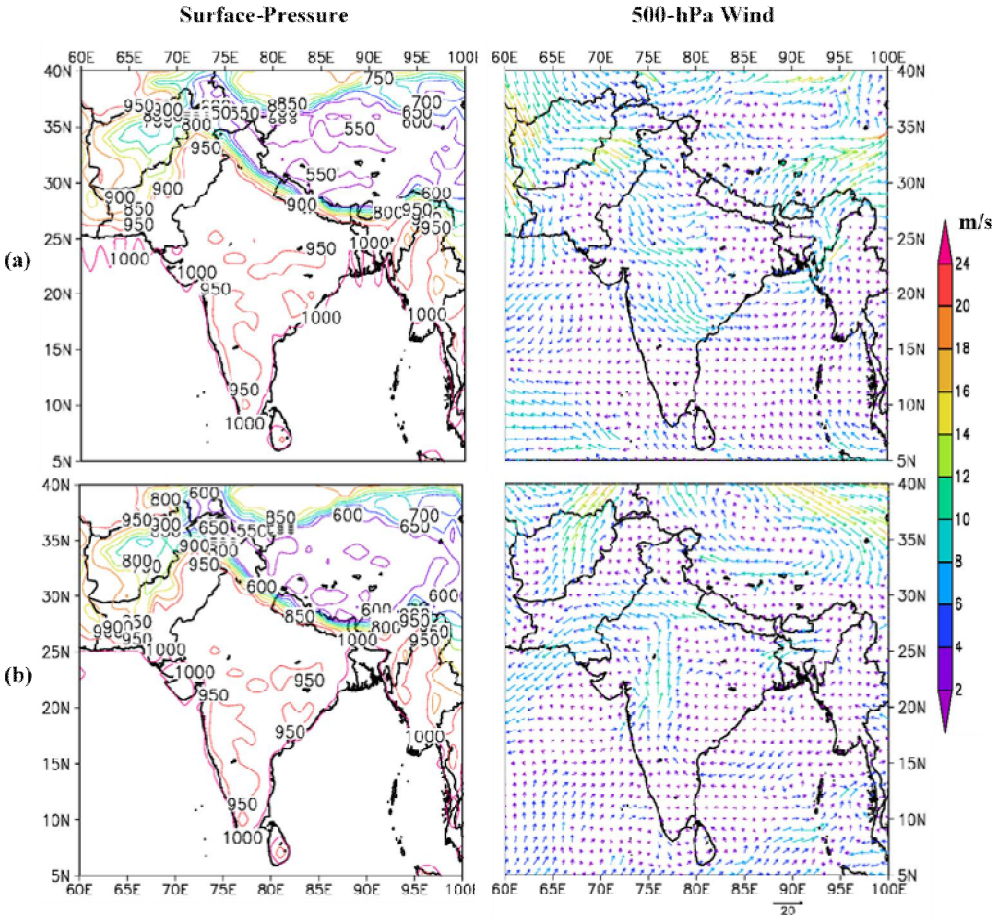

Figure-2: Surface pressure and 500-hPa wind at initial time (00UTC) for (a) 12 July and (b) 14 Aug, 2010.

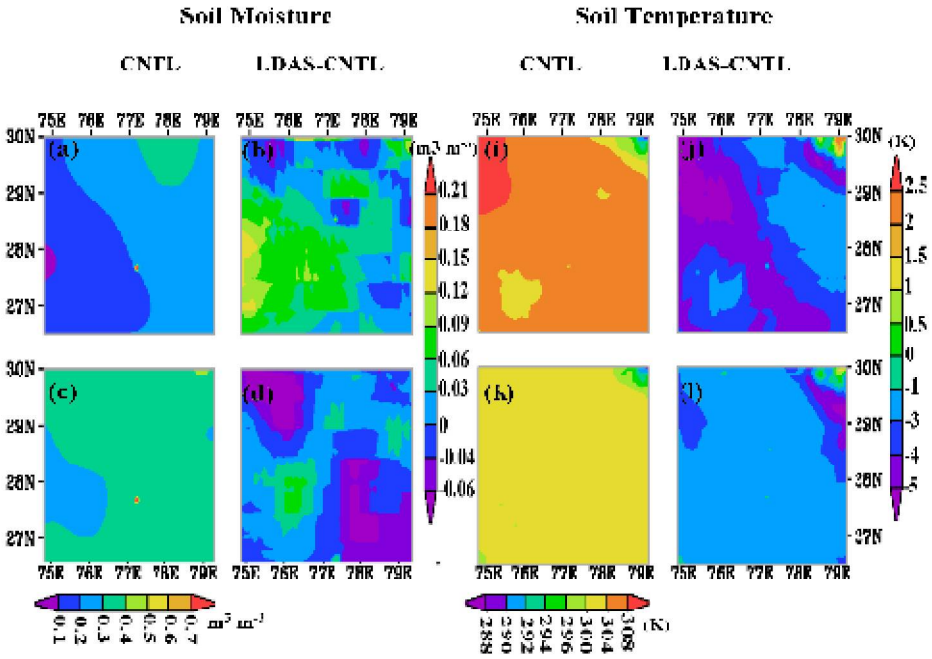

Fig-3: Initial soil moisture availability for (a) CNTL and (b) the difference after using HRLDAS fields (i.e. LDAS-CNTL) for Case-1. (c, d) are same as (a, b) but for case-2. Initial soil temperature for (i) CNTL and (j) the difference after using HRLDAS fields (i.e. LDAS-CNTL) for case-1. (k, l) are same as (i, j) but for case-2.

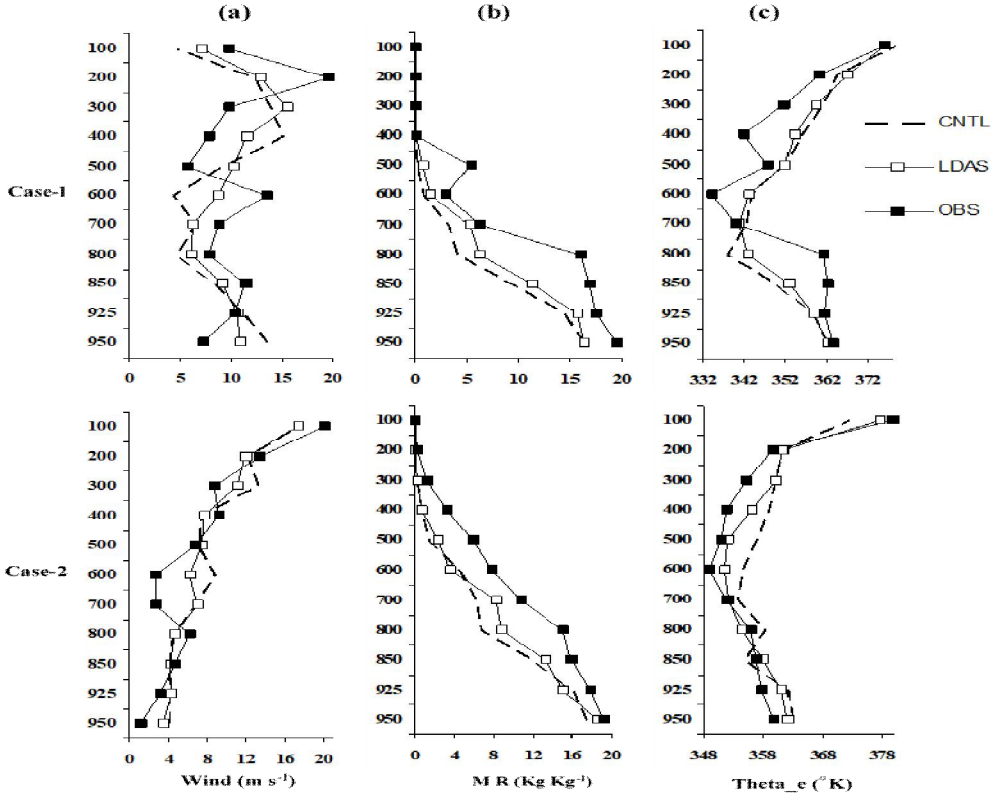

Fig-4: Vertical profile of (a) Wind speed (m/s) and (b) Mixing ratio (g/kg) and (c) Equivalent Potential temperature (°K) from experiments and observation at initial condition over New Delhi.

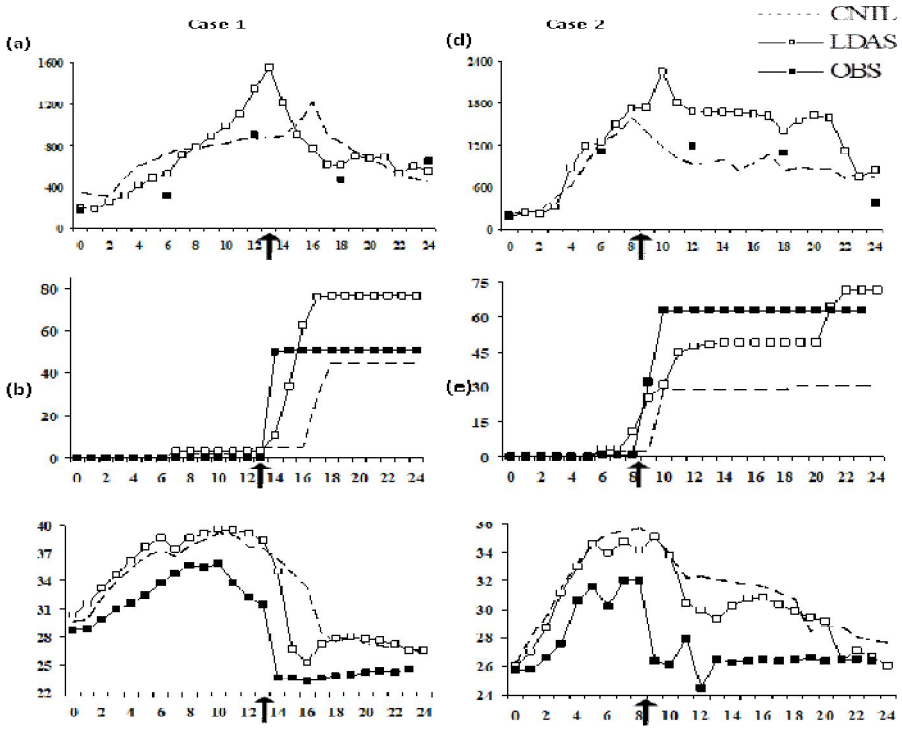

Fig-5: Time series of (a) CAPE J/kg, (b) rainfall (mm) and along with (c) the temperature (°C) over New Delhi for CNTL and LDAS experiment for case-1. (d, e and f) are the same as (a, b and c) but for case-2. Arrow indicates the time of thunderstorm occurrence.

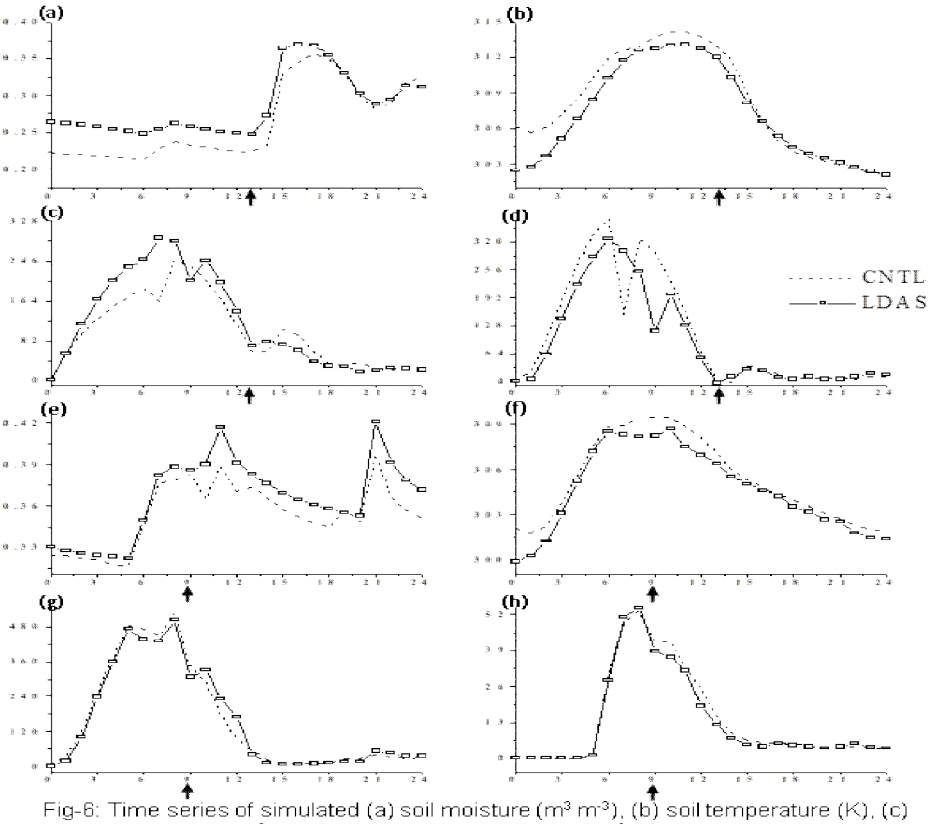

Fig-6: Time series of simulated (a) soil moisture ($m^3\ m^{-3}$), (b) soil temperature (K), (c) latent heat flux ($W m^{-2}$), and (d) sensible heat flux ($W m^{-2}$) for case-1 over New Delhi for CNTL and LDAS experiments. (e – f) are the same as (a-d) but for case-2 for the same station. Arrow indicates the time of thunderstorm occurrence.

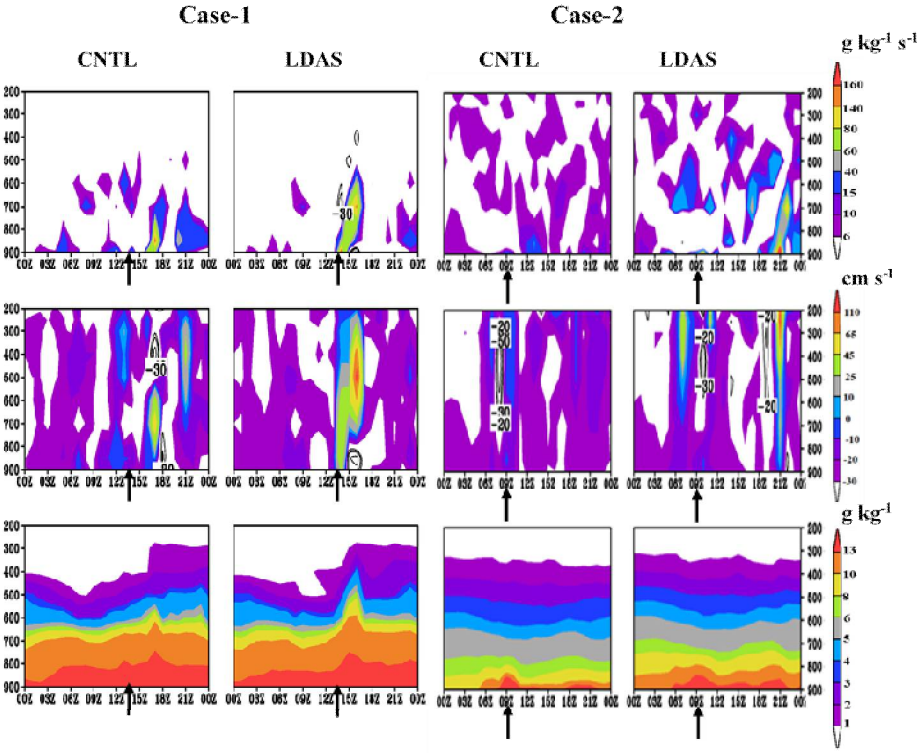

Fig-7: Time-height cross section of (a) moisture convergence, (b) vertical velocity and (c) mixing ratio for case-1 and case-2 for CNTL and LDAS experiments over Delhi. Arrow indicates the time of thunderstorm occurrence.

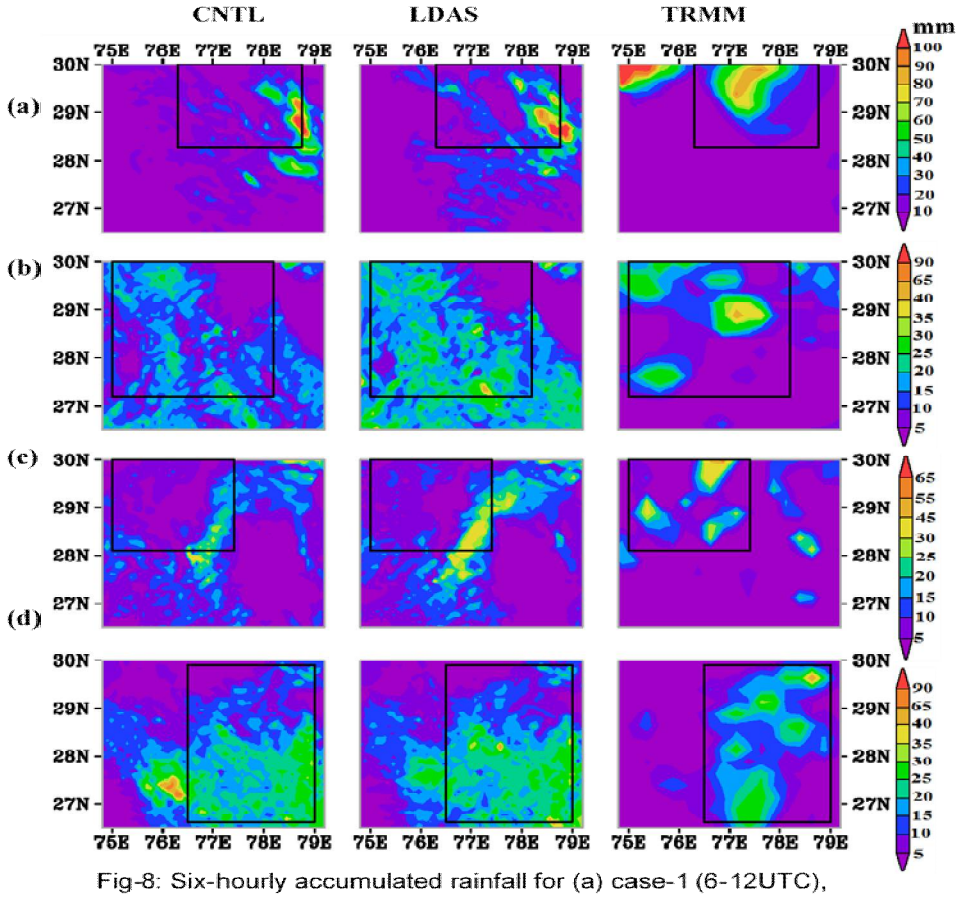

Fig-8: Six-hourly accumulated rainfall for (a) case-1 (6-12UTC), (b) case-2 (12-18UTC) , (c) case-3 (6-12UTC) and (d) case-4 (6-12UTC).

ACKNOWLEDGMENTS

The author acknowledges the financial support provided by DST-SERB (Project Sanction No-EEQ_2017_000206). We also thank the India Meteorological Department (IMD) for providing the observations for model validation. The authors gratefully acknowledge the NCEP/NCAR for making available FNL analysis datasets for the present study. The author is also grateful (GMAO) and GES DISC for providing MERRA and GDAS data respectively.

REFERENCES

1. Wilson, K. B., Baldocchi, D. D., Aubinet, M., Berbigier, P., Bernhofer, C., Dolman, H., Wofsy, S., (2002). Energy partitioning between latent and sensible heat flux during the warm season at FLUXNET sites. Water Resources Research, 38(12), 30-1.
2. Segal, M., Garratt, J. R., Kallos, G., Pielke, R. A. (1989). The Impact of wet soil and canopy temperatures on daytime boundary–layer growth. Journal of Atmospheric Sciences, 46(24), 3673-3684.
3. Eltahir, E. A., Pal, J. S. (1996). Relationship between surface conditions and subsequent rainfall in convective storms. Journal of Geophysical Research: Atmospheres, 101(D21), 26237-26245
4. Bosilovich, M. G., Chern, J. D. (2006). Simulation of water sources and precipitation recycling for the MacKenzie, Mississippi, and Amazon River basins. Journal of Hydrometeorology, *7*(3), 312-329.
5. Barthlott, C., Kalthoff, N. (2011). A numerical sensitivity study on the impact of soil moisture on convection-related parameters and convective precipitation over complex terrain. Journal of the atmospheric sciences, 68(12), 2971-2987.
6. Rajesh, P. V., Pattnaik, S., Rai, D., Osuri, K. K., Mohanty, U. C., Tripathy, S. (2016). Role of land state in a high resolution mesoscale model for simulating the Uttarakhand heavy rainfall event over India. Journal of Earth System Science, 125(3), 475-498.
7. Satyanarayana, A. N. V., Lykossov, V. N., Mohanty, U. C., Machul'Skaya, E. E. (2003). Parameterization of land surface processes to study boundary layer characteristics over a semiarid region in northwest India. Journal of Applied Meteorology, 42(4), 528-540.
8. Hauck, C., Barthlott, C., Krauss, L. and Kalthoff, N., (2011). Soil moisture variability and its influence on convective precipitation over complex terrain. *Quarterly Journal of the Royal Meteorological Society*, *137*(S1), pp.42-56.
9. Dirmeyer, P. A., Halder, S. (2016). Sensitivity of numerical weather forecasts to initial soil moisture variations in CFSv2. Weather and Forecasting, 31(6), 1973-1983.

10. Chandrasekar, A., Alapaty, K., Niyogi, D. (2008). The impacts of indirect soil moisture assimilation and direct surface temperature and humidity assimilation on a mesoscale model simulation of an Indian monsoon depression. *J*ournal of applied meteorology and climatology, 47(5), 1393-1412.
11. Chang, H. I. (2007). Impact of physical parameterization and land use land cover change on the simulation of the July 26, 2005 heavy rain event over Mumbai, India. In 21st Conference on Hydrology.
12. Ma, W., Ma, Y. (2016). Modeling the influence of land surface flux on the regional climate of the Tibetan Plateau. Theoretical and Applied Climatology, 125(1), 45-52.
13. Osuri, K. K., Nadimpalli, R., Mohanty, U. C., Chen, F., Rajeevan, M., Niyogi, D. (2017). Improved prediction of severe thunderstorms over the Indian Monsoon region using high-resolution soil moisture and temperature initialization. Scientific Reports, 7(1), 1-12.
14. Ek, M. B., Mitchell, K. E., Lin, Y., Rogers, E., Grunmann, P., Koren, V., ... & Tarpley, J. D. (2003). Implementation of Noah land surface model advances in the National Centers for Environmental Prediction operational mesoscale Eta model. *Journal of Geophysical Research: Atmospheres*, *108*(D22).
15. Tewari, M., Chen, F., Wang, W., Dudhia, J., LeMone, M. A., Mitchell, K., ... & Cuenca, R. H. (2005), January. Numerical experiments with upgraded WRF/NoahLSM model. In Preprints of the Proceedings 19th Conference on Hydrology, San Diego, CA, Am. Meteorol. Soc.(http://ams. confex. com/ams/pdfpapers/87342. Pdf).
16. Pielke, R. A. (1974). A comparison of three-dimensional and two-dimensional numerical predictions of sea breezes. Journal of Atmospheric Sciences, 31(6), 1577-1585.
17. Tapp, M. C., White, P. W. (1976). A non-hydrostatic mesoscale model. Quarterly Journal of the Royal Meteorological Society, 102(432), 277-296.
18. Anthes, R. A., Warner, T. T. (1978). Development of hydrodynamic models suitable for air pollution and other mesometerological studies. Monthly Weather Review, 106(8), 1045-1078.
19. Deardorff, J. W. (1978). Efficient prediction of ground surface temperature and moisture, with inclusion of a layer of vegetation. Journal of Geophysical Research: Oceans, 83(C4), 1889-1903.
20. Lewis, J. M., Derber, J. C. 1985. The use of adjoint equations to solve a variational adjustment problem with advective constraints. Tellus A, 37(4), 309-322.
21. McNally, A. P. (2002). A note on the occurrence of cloud in meteorologically sensitive areas and the implications for advanced infrared sounders. Quarterly Journal of the Royal Meteorological Society: A journal of the atmospheric sciences, applied meteorology and physical oceanography, 128(585), 2551-2556.
22. Sikora, C. R. (1976). *An Investigation of Equivalent Potential Temperature as a Measure of Tropical Cyclone Intensity*. Fleet Weather Central/Joint Typhoon Warning Center FPO San Francisco 96630.
23. Price, C. (2006). Global thunderstorm activity. In Sprites, elves and intense lightning discharges (pp. 85-99). Springer, Dordrecht.
24. Rasmussen, E.N. and Wilhelmson, R.B., (1983). Preprints, 13th Conference on Severe Local Storms..
25. López, L., García-Ortega, E., Sánchez, J. L. 2007. A short-term forecast model for hail. Atmospheric research, *83*(2-4), 176-184.
26. Flerchinger, G. N., Saxton, K. E. (1989). Simultaneous heat and water model of a freezing snow-residue-soil system II. Field verification. *Transactions of the ASAE*, *32*(2), 573-0576.
27. Flerchinger, G. N., Kustas, W. P., Weltz, M. A. (1998). Simulating surface energy fluxes and radiometric surface temperatures for two arid vegetation communities using the SHAW model. *Journal of Applied Meteorology*, *37*(5), 449-460.
28. Guo, D., Yang, M., Wang, H. (2011). Characteristics of land surface heat and water exchange under different soil freeze/thaw conditions over the central Tibetan Plateau. Hydrological Processes, *25*(16), 2531-2541.
29. Zipser, E. J., Cecil, D. J., Liu, C., Nesbitt, S. W., Yorty, D. P. (2006). Where are the most intense thunderstorms on Earth?. Bulletin of the American Meteorological Society, 87(8), 1057-1072.
30. Kirkpatrick, C., McCaul Jr, E. W., Cohen, C. (2009). Variability of updraft and downdraft characteristics in a large parameter space study of convective storms. Monthly Weather Review, 137(5), 1550-1561.
31. Yin, Z. Y., Zhang, X., Liu, X., Colella, M., Chen, X. (2008). An assessment of the biases of satellite rainfall estimates over the Tibetan Plateau and correction methods based on topographic analysis. Journal of Hydrometeorology, 9(3), 301-326.
32. Maussion, F., Scherer, D., Finkelnburg, R., Richters, J., Yang, W. and Yao, T., (2011). WRF simulation of a precipitation event over the Tibetan Plateau, China–an assessment using remote sensing and ground observations. *Hydrology and Earth System Sciences*, *15*(6), pp.1795-1817.

CITATION OF THIS ARTICLE

N Verma, S Kundan, Z Nabi, D Kumar. Soil moisture and soil temperature assimilation using HRLDAS for heavy rainfall event forecasting over the Indian region. Bull. Env.Pharmacol. Life Sci., Vol 11 [11] October 2022 :204-214